

# EXAFS and XRD investigations of zeunerite and meta-zeunerite

C. Hennig<sup>\*I</sup>, G. Reck<sup>II</sup>, T. Reich<sup>I</sup>, A. Roßberg<sup>I</sup>, W. Kraus<sup>II</sup> and J. Sieler<sup>III</sup>

<sup>I</sup> Forschungszentrum Rossendorf, Institut für Radiochemie, PF 51 01 19, D-01314 Dresden, Germany

<sup>II</sup> Bundesanstalt für Materialforschung und -prüfung, Richard-Willstätter-Str. 11, D-12489 Berlin, Germany

<sup>III</sup> Universität Leipzig, Institut für Anorganische Chemie, Linnéstr. 3, D-04103 Leipzig, Germany

Received June 22, 2001; accepted July 8, 2002

**Abstract.** In this paper EXAFS was used to determine bond lengths in the structures of zeunerite and meta-zeunerite. The atomic distances between heavy and light scatterers observed using EXAFS in meta-zeunerite deviate approximately 0.1 Å from literature data of single-crystal X-ray diffraction measurements. Because this difference is significant higher than the error limits of EXAFS measurements, the complete crystal structure of meta-zeunerite,  $\text{Cu}[\text{UO}_2\text{AsO}_4]_2 \cdot 8 \text{H}_2\text{O}$ , is revised by X-ray structure analysis. The bond length determinations by EXAFS and the revised XRD data agree within the experimental error limits. In this study EXAFS spectroscopy has proven to be an useful tool for determining precise local bond lengths in the environment of heavy atoms. Moreover, the crystal structure of zeunerite,  $\text{Cu}[\text{UO}_2\text{AsO}_4]_2 \cdot 12 \text{H}_2\text{O}$ , hitherto not been described in the literature, was investigated. Reflex broadening effects and intergrowth relationship between zeunerite and meta-zeunerite show that meta-zeunerite grows in nature due to dehydration of zeunerite. The structural transition from zeunerite to meta-zeunerite is connected with a change in the uranyl arsenate layer arrangement and the crystal water content.

## 1. Introduction

X-ray diffraction (XRD) techniques allow a precise analysis of crystal structures. With modern equipment, even hydrogen atoms can be determined adjacent to heavy atoms. However, in the presence of very heavy atoms, crystal structure determination by single-crystal X-ray diffraction measurements is sometimes less accurate. The reflection intensities are mainly influenced by the heavy scatterers and the error in atomic coordinates increases for the light atoms. The difficulties increase if only crystals of poor quality are available or problems in symmetry determination appear. In these cases, a bond length determination independent from crystal quality and the knowledge of lattice parameters is helpful. Extended X-ray Absorption Fine Structure (EXAFS) spectroscopy allows determining the distances between heavy atoms and the immediately surrounding atoms. The estimated standard deviations for

bond lengths are less than 0.02 Å; the accuracy decreases for more distant shells. EXAFS gives only the average bond length in each single coordination shell. As shown in this paper, the atomic distances determined by EXAFS on natural meta-zeunerite deviate considerably from the single crystal structure data of Hanic [1]. Similar differences between EXAFS and XRD measurements for other uranium compounds are described in the literature [2]. For this reason and taking into account that Hanic [1] could use only intensities from Weissenberg photographs for his structure analysis, a complete redetermination of the meta-zeunerite structure was carried out. EXAFS was used furthermore to distinguish structural differences between zeunerite and meta-zeunerite. The crystal structure of zeunerite is described here for the first time.

Zeunerite and meta-zeunerite are secondary grown minerals, which arise from uranium and arsenic primary minerals in the oxidized zone of rock deposits. They belong to the structure family with the chemical formula  $\text{A}^{m+}[\text{UO}_2\text{XO}_4]_m \cdot n \text{H}_2\text{O}$ , where  $\text{XO}_4$  appears as phosphate or arsenate and A is a hydrated monovalent or divalent cation [3, 4]. In nature, both A and X occur often mixed by isomorphous replacement. Because of the wide range of the interlayer cations  $\text{A}^{m+}$ , this group includes a lot of structurally related members [5]. The main structural principles are well known [3] and will be summarized here shortly. Each  $[\text{UO}_2]^{2+}$  unit is built up by uranium with two double bonded oxygen atoms in axial direction ( $\text{O}_{\text{ax}}$ ). This uranyl unit is surrounded in the equatorial plane by four oxygen atoms ( $\text{O}_{\text{eq}}$ ) in a square planar arrangement. Tetrahedra of  $[\text{XO}_4]^{3-}$  ions and tetragonal dipyramidal coordinated uranyl ions  $[\text{UO}_2]^{2+}$  build stable layers. These  $[\text{UO}_2\text{XO}_4]_{\infty}$  layers are connected forming crystals with a tetragonal or pseudotetragonal morphology and a platy (001) habit. The uranyl arsenate layer structure causes perfect cleavage. Charge neutrality of the uranyl arsenate layers is given by hydrated  $[\text{A}(\text{H}_2\text{O})_4]^{m+}$  cations.

Zeunerite and meta-zeunerite are two different hydrates of copper uranyl arsenate. The interlayer water content varies depending on vapor pressure and temperature. Three stable hydrate species of  $\text{Cu}[\text{UO}_2\text{AsO}_4]_2 \cdot n \text{H}_2\text{O}$  have been described [6, 7]: (i) the completely hydrated phase, zeunerite, with  $n = 12 \text{H}_2\text{O}$ , (ii) meta-I hydrate containing  $n = 8 \text{H}_2\text{O}$ , naturally occurring as meta-zeunerite and (iii) meta-II hydrate containing  $n = 2-5 \text{H}_2\text{O}$ .

\* Correspondence author (e-mail: C.Hennig@fz-rossendorf.de)

Meta-II hydrate is only recognized under laboratory conditions but does not occur naturally. There are more dehydration stages proposed in the meta-II hydrate region [8]. The transition between the completely hydrated phase and the meta-I hydrate occurs near ambient temperatures and at low humidity during a long time. At 55 °C the transition from zeunerite to meta-zeunerite happens within two hours [7]. Problems concerning the determination of the crystal symmetry and crystal structure may occur, especially if two hydrate species co-exist. According to the tetragonal crystal symmetry, zeunerite and meta-zeunerite should be optically uniaxial. Weak deviations from expected uniaxial behavior were described for rare cases. Deviations from uniaxial optic are very small for meta-zeunerite. An optical axis angle of maximal  $2V = 8^\circ$  for zeunerite is mentioned [7], which probably arises from a hydrate transition state. But this has not been confirmed by X-ray diffraction methods.

In a first step, the EXAFS results estimated on zeunerite/meta-zeunerite will be represented. Deviations of the obtained bond lengths from X-ray diffraction literature data [1] will be discussed. In a second step, the single crystal structure analysis on zeunerite and meta-zeunerite will be described and compared with the EXAFS results.

## 2. Experimental

### 2.1. Samples

Natural zeunerite/meta-zeunerite often contains phosphate as isomorphous replaced element instead of arsenate. Therefore, two samples from a collection of different zeunerite minerals were selected with a negligible phosphorus content ascertained by microprobe analysis. The phase content was analyzed by powder X-ray diffraction. An intergrown zeunerite/meta-zeunerite mineral from Wheal Basset, Cornwall/England (sample 1) was used for EXAFS, powder and single-crystal X-ray diffraction measurements. It should be noted that the zeunerite content in this sample can be ignored for EXAFS measurements. A pure zeunerite crystal fragment was separated for XRD measurements from the same sample. An additional sample of meta-zeunerite from the mine "Weißer Hirsch", Schneeberg/Saxony in Germany, (sample 2) consisting of very small crystals was used for single-crystal X-ray diffraction measurements. Furthermore, an attempt was made to obtain single crystals by synthesis according to the procedure described in the literature [8]. The resulting compound (sample 3) has been proven by powder X-ray diffraction to be identical with zeunerite,  $\text{Cu}[\text{UO}_2\text{AsO}_4]_2 \cdot 12 \text{H}_2\text{O}$ . Because no single crystals were obtained by synthesis, sample 3 was used only for low-temperature Cu K-edge EXAFS measurements.

### 2.2. EXAFS measurements

EXAFS measurements were carried out on the Rossendorf Beamline (ROBL) [9] at the European Synchrotron Radiation Facility (ESRF) under dedicated ring conditions (6.0 GeV, 100–200 mA). The monochromator, which is

equipped with a water-cooled Si(111) double-crystal system, was used in channel-cut measuring mode. Higher harmonics were rejected by two Pt coated mirrors. The first mirror collimates the X-ray beam onto the monochromator crystal. The second mirror focuses the beam vertically to the sample. The vertical slit aperture before the sample was set to 0.8 mm. A monochromator feedback control system [10] was used for suppressing the decay of the primary X-ray flux. Energy steps were calculated giving corresponding  $k$ -space steps of  $0.05 \text{ \AA}^{-1}$ . The sample was sealed with polyethylene foil for safety reasons. All measurements were taken at ambient conditions with the exception of two spectra measured at the Cu–K edge. Samples 1 and 3 were ground in an agate mortar, mixed with boron nitride and pressed as 1.3 cm diameter pellet. The amount of uranium used was calculated to give a jump of one across the uranium  $L_{\text{III}}$ -edge. The same sample was used for the As K-edge and for the Cu K-edge measurements. Uranium  $L_{\text{III}}$ -edge and arsenic K-edge EXAFS were collected in transmission geometry using argon-filled ionization chambers. Two scans were recorded for each energy range, and the spectra were averaged. The copper K-edge EXAFS spectrum at room temperature was measured in fluorescence mode using a four-pixel Ge detector [11]. In order to distinguish structural differences between  $\text{Cu}[\text{UO}_2\text{AsO}_4]_2 \cdot 12 \text{H}_2\text{O}$  and  $\text{Cu}[\text{UO}_2\text{AsO}_4]_2 \cdot 8 \text{H}_2\text{O}$  by reducing thermal oscillations through cooling the samples to 15 K, a closed-cycle He cryostat was used. Eight single scans were averaged for the Cu K-edge fluorescence spectrum measured at  $T = 298 \text{ K}$ . For the measurements at  $T = 15 \text{ K}$ , only two scans were used. Sample orientation during the fluorescence measurements was  $45^\circ$  to the beam. Because of the polarization dependence, transmission measurements were carried out using a sample with a normal orientation of  $0^\circ$  and  $45^\circ$  to the beam direction. Metal foils were used to provide energy calibration references. First inflection points at the Zr K-edge at 17995.9 eV and at the Au  $L_{\text{III}}$ -edge at 11919.7 eV [12] were used for energy calibration. EXAFS data was extracted from the raw absorption spectra by standard methods using the computer program EXAFSPAK [13].

### 2.3. X-ray diffraction measurements

In order to ascertain the relation of zeunerite and meta-zeunerite in sample 1, a quantitative phase analysis from X-ray powder diffraction measurement was carried out with the program PowderCell [14]. For this measurement a quartz capillary with a diameter of 0.3 mm was filled with a fine powder of sample 1. The powder pattern was recorded on a STOE StadiP transmission diffractometer in Debye-Scherrer geometry using  $\text{CuK}_\alpha$  radiation ( $\lambda = 1.5405 \text{ \AA}$ ) in a  $2\theta$  range of  $5^\circ$  to  $100^\circ$  with a step width of  $0.02^\circ$ . The intergrowth relationship between zeunerite and meta-zeunerite in sample 1 was identified by Weissenberg photographs. This measurement was performed using unfiltered Cu radiation. Intensity data for single-crystal analyses were collected on a Siemens SMART three-circle diffractometer equipped with a CCD area detector. Details of data collection for the crystal structure determination of zeunerite and meta-zeunerite are listed in Table 1. The first

**Table 1.** Details of data collection, structure determination and crystallographic data of zeunerite and meta-zeunerite. Estimated standard deviations are given in parentheses.

Mineral	Zeunerite	Meta-zeunerite (ordered)	Meta-zeunerite (disordered)
Formula	Cu[ $\text{UO}_2\text{AsO}_4$ ] <sub>2</sub> · 12 H <sub>2</sub> O	Cu[ $\text{UO}_2\text{AsO}_4$ ] <sub>2</sub> · 8 H <sub>2</sub> O	
Crystal system	tetragonal	tetragonal	
Space group	<i>I4/mmm</i>	<i>P4/ncc</i>	<i>P4/nmm</i>
	(No. 139)	(No. 130 2)	(No. 129 2)
Lattice constants a [Å]	7.1751(3)	7.1065(6)	7.1065(6)
c [Å]	20.8728(12)	17.4195(11)	8.7095(11)
V [Å <sup>3</sup> ]	1074.57(9)	879.73(12)	439.85(8)
Z	2	2	1
<i>d</i> <sub>calculated</sub> [g · cm <sup>-3</sup> ]	3.392	3.872	3.872
Absorption $\mu$ [mm <sup>-1</sup> ]	19.173		23.390
<i>F</i> (000)	990	910	455
Crystal size [mm <sup>3</sup> ]	0.10 × 0.05 × 0.02		0.10 × 0.07 × 0.02
Diffractometer	Siemens SMART with CCD area detector		
Radiation/ $\lambda$ [Å]	MoK $\alpha$ /0.71073		
Temperature [K]	293		
Scan mode	$\omega$		
2 $\theta$ range [°]	8.85–7.6	7.45–7.4	
Index ranges	–9 ≤ <i>h</i> ≤ 9 –9 ≤ <i>k</i> ≤ 9 –15 ≤ <i>l</i> ≤ 28	–8 ≤ <i>h</i> ≤ 9 –9 ≤ <i>k</i> ≤ 9 –23 ≤ <i>l</i> ≤ 13	–8 ≤ <i>h</i> ≤ 9 –9 ≤ <i>k</i> ≤ 9 –11 ≤ <i>l</i> ≤ 6
No. of reflections measured	3104	3638	2352
unique	400	506	352
Absorption correction		semi-empirical $\psi$ -scan	
Structure solutions		SHELX-97	
Parameters refined	27	29	34
<i>R</i> 1 (on <i>F</i> )	0.037	0.056	0.029
<i>wR</i> 2 (on <i>F</i> <sup>2</sup> )	0.085	0.132	0.072
Goodness of Fit	1.04	0.87	0.87
$\Delta Q_{\text{max}}$ [e · Å <sup>-3</sup> ]	1.11	0.99	0.96
$\Delta Q_{\text{min}}$ [e · Å <sup>-3</sup> ]	–1.63	–1.02	–1.82

crystal piece investigated from sample **1** contained zeunerite and meta-zeunerite so that the *hk0* reflections of both phases coincided completely. Some *hkl* reflections are partly overlapped. Nevertheless, both crystal structures could be identified. In order to achieve a better comparison of bond lengths obtained by X-ray diffraction and EXAFS measurements, a piece consisting exclusively of zeunerite was separated from the center of a large crystal from sample **1**. Because of the better crystal quality, the results for meta-zeunerite obtained from sample **2** are presented here. Both structures were solved by direct methods and difference Fourier syntheses. Atomic coordinates and anisotropic displacement parameters were refined by full-matrix least-squares calculations<sup>1</sup>.

### 3. Results and discussions

#### 3.1. EXAFS investigations

To find a set of characteristic bond lengths, the EXAFS spectra were measured at the U L<sub>III</sub>-edge, at the As K-

edge and at the Cu K-edge. Fourier transforms (FT) of the EXAFS signals represent radial distribution functions of the near-neighbors around the absorber atom. The FT peaks appear at lower R values relative to the true near-neighbor distances as an effect of the EXAFS phase shift. This phase shift influences the bond length determination by additional terms  $\Delta$ , which are different for each neighboring atom. The program FEFF8 [15] was used to calculate theoretical backscattering phase and amplitude functions. This theoretical approach describes the photoelectron final states by an *ab initio* curved-wave multiple-scattering calculation using an energy-dependent muffin-tin potential. Final-state potentials were calculated using atomic clusters derived from the known atomic coordinates of uranyl arsenate structures as referred in [16]. The phase and amplitude functions were determined by U L<sub>III</sub>-edge scattering potentials approximated with 52 atoms in a 16-shell cluster with a radius of 5.4 Å. Phase and amplitude functions for the scattering pairs As–O<sub>eq</sub> and As–U were determined using a cluster with a radius of 4.6 Å. In solid samples the coordination numbers are influenced by polarization effects due to the preferred orientation of the crystallites. The preferred orientation is caused by uniaxial pressure during sample preparation as described in [17]. The atomic distances can be also slightly influenced by the effects of polarization [18]. In order to investigate the influence of polarization effects on the reliability of the determined values, the transmission experiments were performed at two different sample orientations.

<sup>1</sup> Additional material to this paper can be ordered referring to the no. CSD 412820 (As<sub>2</sub>CuH<sub>24</sub>O<sub>24</sub>U<sub>2</sub>), CSD 412821 (As<sub>2</sub>CuH<sub>16</sub>O<sub>20</sub>U<sub>2</sub>/m-zeu130), and CSD 412822 (As<sub>2</sub>CuH<sub>16</sub>O<sub>20</sub>U<sub>2</sub>/m-zeu129), names of the authors and citation of the paper at the Fachinformationszentrum Karlsruhe, Gesellschaft für wissenschaftlich-technische Information mbH, D-76344 Eggenstein-Leopoldshafen, Germany. The list of *F*/*F*<sub>c</sub>-data is available from the author up to one year after the publication has appeared.

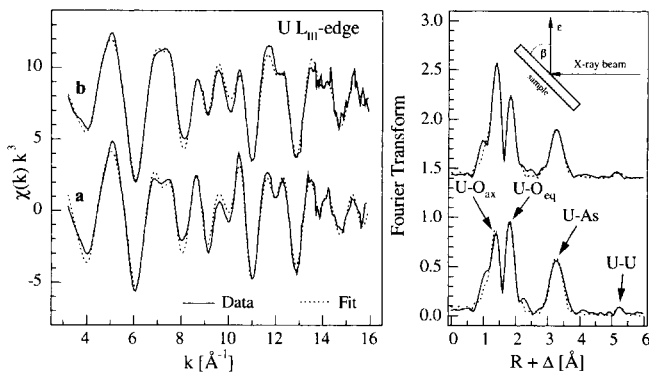


**Fig. 1.** U L<sub>III</sub>-edge  $k^3$ -weighted EXAFS spectra of copper uranyl arsenate sample **1** (left) and the corresponding Fourier transforms (right) with  $\beta = 0^\circ$  (a) and  $\beta = 45^\circ$  (b) measured at  $T = 298$  K. The angle  $\beta$  is defined as tilt angle between the sample surface and the polarization vector  $\epsilon$ .

### 3.1.1. Uranium L<sub>III</sub>-edge EXAFS

Uranium  $k^3$ -weighted polarization dependent EXAFS spectra of sample **1** are shown in Fig. 1. Measurements were carried out using two sample orientations, given by the tilt angle  $\beta$ . This angle is defined as the angle between the polarization vector  $\epsilon$  and the sample surface (see Fig. 1). Structural parameters obtained from the fit procedures are given in Table 2. FT features in the figures are uncorrected for phase shifts. In the U L<sub>III</sub>-edge FT, the first shell represents the axial oxygen atoms, O<sub>ax</sub>, at a distance of 1.77–1.79 Å. The smallest resolvable difference in interatomic distances for two different bond lengths in EXAFS measurements is given by the ratio  $\Delta R = \pi/(2 \Delta k)$ , where  $\Delta k$  is the  $k$ -range of the fitted data. For the  $k$ -range of 13 Å<sup>-1</sup> used for the U L<sub>III</sub>-edge spectra, the resolution  $\Delta R$  is 0.12 Å. However, the expected U–O<sub>ax</sub> bond length differences are not sufficiently large that they could be refined in the least-square fit without constraining some fit parameters. The average U–O<sub>ax</sub> bond distance given by EXAFS is around 0.1 Å shorter than the averaged value of the axial bond distances 1.94 Å and 1.78 Å reported in the literature [1]. The sec-

ond shell in the FT corresponds to the bond distance of four symmetry-equivalent equatorial atoms (O<sub>eq</sub>) with a bond length of 2.29 Å. For comparison, the corresponding value given in [1] is 2.18 Å. The coordination numbers for the axial oxygen atoms, N<sub>O<sub>ax</sub></sub>, and for the equatorial oxygen atoms, N<sub>O<sub>eq</sub></sub>, deviate significantly from the expected values. This is due to polarization effects in the EXAFS signal and caused by the preferred orientation of the uranyl arsenate layers with respect to the X-ray beam direction. For a tilt angle  $\beta = 0^\circ$  the coordination number N<sub>O<sub>ax</sub></sub> is 1.6 and N<sub>O<sub>eq</sub></sub> is 4.5 atoms. N<sub>O<sub>ax</sub></sub> is lower and N<sub>O<sub>eq</sub></sub> is higher than the crystallographic value. At a tilt angle  $\beta = 45^\circ$  the relation is reversed. The coordination number N<sub>O<sub>ax</sub></sub> is 2.2 and N<sub>O<sub>eq</sub></sub> is 3.2. Scattering from the arsenic atoms contributes to a significant third FT peak with a calculated U–As distance of 3.69–3.70 Å. The U–U scattering contribution generates a very weak FT peak corresponding to a bond length of 5.40–5.44 Å. These distances between heavy scatterers agree within the error limits with the values described in the literature (U–As = 3.68 Å and U–U = 5.38 Å) [1]. A scattering contribution from copper and oxygen atoms in the interlayer [Cu(H<sub>2</sub>O)<sub>4</sub>]<sup>2+</sup> group was not detectable because amplitude damping effects increase with increasing distances. These results demonstrate that polarization effects influence the coordination numbers but do not significantly affect the distances measured by EXAFS. Thus, within the typical error limits the preferred orientation does not limit the determination of distances.

### 3.1.2. As K-edge

EXAFS measurements with As as absorbing atom are shown in Fig. 2. Due to the [AsO<sub>4</sub>] tetrahedral coordination geometry, polarization effects do not occur. The arsenate tetrahedra have an As–O<sub>eq</sub> bond length of 1.68 Å. The As–U distance is 3.683–.70 Å. The As–O<sub>eq</sub> distance given in [1] is 1.77 Å. It follows from the comparison of the EXAFS and XRD that only the bond distances to the surrounding oxygen atoms differ significantly whereas the

Edge, $\beta$	Shell	R <sub>EXAFS</sub> [Å] <sup>a</sup>	N <sup>b</sup>	$\sigma^2$ [Å <sup>2</sup> ]	$\Delta E_0$ [eV]	Error	R <sub>XRD</sub> [Å]
U L <sub>III</sub> , 0°	U–O <sub>ax</sub>	1.77	1.6(1)	0.0021	0.1	0.23	1.94, 1.78
	U–O <sub>eq</sub>	2.29	4.5(1)	0.0035			
	U–As	3.70	2.7(2)	0.0039			
	U–U	5.44	2.2(7)	0.0079			
U L <sub>III</sub> , 45°	U–O <sub>ax</sub>	1.79	2.2(1)	0.0024	1.1	0.19	
	U–O <sub>eq</sub>	2.29	3.2(1)	0.0028			
	U–As	3.69	2.0(2)	0.0035			
	U–U	5.40	1.9(6)	0.008 <sup>c</sup>			
As K, 0°	As–O <sub>eq</sub>	1.68	5.1(1)	0.0025	-7.2	1.10	1.77
	As–U	3.68	2.8(3)	0.0042			
As K, 45°	As–O <sub>eq</sub>	1.68	5.0(1)	0.0022	-5.9	0.92	
	As–U	3.70	1.4(2)	0.0025			
Cu K, 45°	Cu–O	1.95	2.9(1)	0.0029	-5.2	0.58	2.14

**Table 2.** EXAFS structural parameters for the copper uranyl arsenate sample **1**. For comparison the atomic bond distances R<sub>XRD</sub> from literature [1], at 298 K.

a: Errors in distances R are  $\pm 0.02$  Å

b: Errors in coordination numbers N are  $\pm 25\%$  with standard deviations in parentheses,  $\sigma^2$  – Debye-Waller factor,  $\beta$  – angle between polarization vector  $\epsilon$  and sample surface (see Fig. 1).

c: Value fixed during the fit

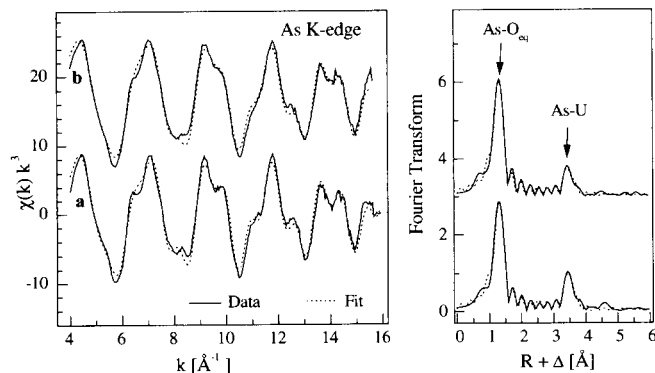


**Fig. 2.** As K-edge  $k^3$ -weighted EXAFS spectra of copper uranyl arsenate sample **1** (left) and the corresponding Fourier transforms (right) with  $\beta = 0^\circ$  (a) and  $\beta = 45^\circ$  (b) measured at  $T = 298$  K.

As–U distances are in agreement. The distances to the heavy scatterers in meta-zeunerite were the subject of a more detailed study using low-temperature EXAFS measurements at the U L<sub>III</sub>- and As K-edges [19]. Both the measurements at the U L<sub>III</sub>-edge and at the As K-edge detected atomic distances within the  $[\text{UO}_2\text{AsO}_4]_\infty$  layer only.

### 3.1.3. Cu K-edge

The Cu–O distance was determined from Cu K-edge EXAFS (Fig. 3). Merely one peak is visible in the FT at room temperature. To calculate Cu–O phase and amplitude functions, a simple one-shell cluster was built using the atomic coordinates for the  $[\text{Cu}(\text{H}_2\text{O})_4]^{2+}$  group in meta-torbernite [20]. For the copper uranyl arsenate sample **1**, the least square fit gave an average Cu–O bond length of 1.95  $\text{\AA}$ . This value reflects predominantly the scattering contributions from the coordinated water in the  $[\text{Cu}(\text{H}_2\text{O})_4]^{2+}$  group. No contribution of the O<sub>ax</sub> atoms, which are expected at 2.5  $\text{\AA}$ , could be observed in the FT. The Cu–O distance in the  $[\text{Cu}(\text{H}_2\text{O})_4]^{2+}$  group measured by XRD is 2.14  $\text{\AA}$  [1]. For comparison, the Cu–O bond length in the isostructural mineral meta-torbernite,  $\text{Cu}[\text{UO}_2\text{PO}_4]_2 \cdot 8 \text{H}_2\text{O}$ , is 1.92  $\text{\AA}$  [20].

Low-temperature Cu K-edge EXAFS measurements at 15 K were performed to study the main structural difference between  $\text{Cu}[\text{UO}_2\text{AsO}_4]_2 \cdot 12 \text{H}_2\text{O}$  and  $\text{Cu}[\text{UO}_2\text{AsO}_4]_2 \cdot 8 \text{H}_2\text{O}$ . Sample **1** was representative for  $\text{Cu}[\text{UO}_2\text{AsO}_4]_2 \cdot 8 \text{H}_2\text{O}$  and sample **3** for  $\text{Cu}[\text{UO}_2\text{AsO}_4]_2 \cdot 12 \text{H}_2\text{O}$ , respectively. Cu

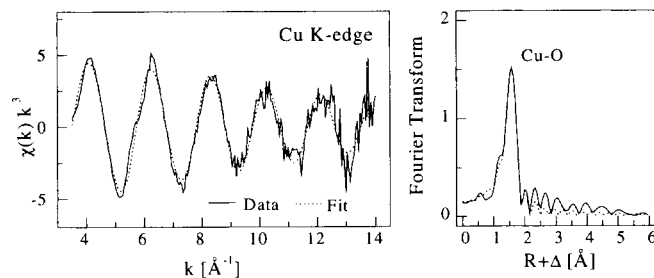


**Fig. 3.** Cu K-edge  $k^3$ -weighted EXAFS spectra of copper uranyl arsenate sample **1** (left) and the corresponding Fourier transform (right) with  $\beta = 45^\circ$  measured at  $T = 298$  K.

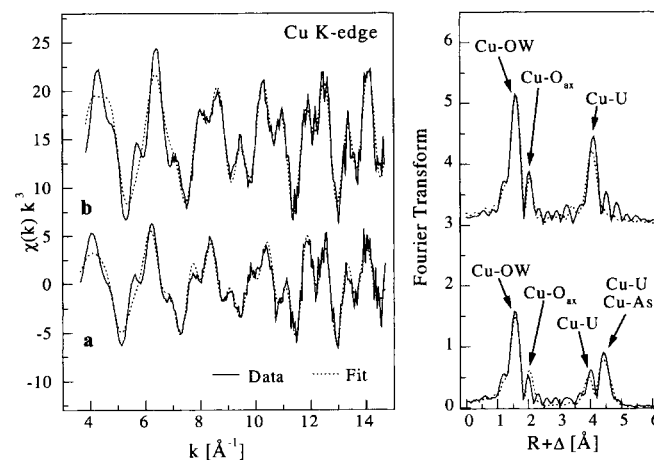


**Fig. 4.** Cu K-edge  $k^3$ -weighted EXAFS spectra (left) and the corresponding Fourier transforms (right) with  $\beta = 45^\circ$  of sample **1** (a) and sample **3** (b) measured at  $T = 15$  K.

K-edge EXAFS spectra at low temperature are shown in Fig. 4 and the fit results are given in Table 3. Due to the damping of thermal oscillations at 15 K, additional backscattering shells occur in the FT (compare Figs. 3 and 4). To simplify the data analysis, the FT between  $R + \Delta = 5.5\text{--}10 \text{\AA}$  was Fourier filtered, back transformed and subtracted from raw EXAFS data. The  $[\text{Cu}(\text{H}_2\text{O})_4]^{2+}$  group causes dominant FT peaks with Cu–O distances of 1.94  $\text{\AA}$  for both samples **1** and **3**. The scattering contribution of O<sub>ax</sub> gives a weak peak at a distance of 2.46  $\text{\AA}$ . Sample **3** shows one Cu–U peak at a distance of 4.22  $\text{\AA}$ . A strong Cu–U–O<sub>ax</sub>–Cu MS contribution appears in the FT of sample **3** due to the linear arrangement of the corresponding atoms. This observation points

**Table 3.** Cu K-edge EXAFS structural parameters for sample **1**, meta-zeunerite,  $\text{Cu}[\text{UO}_2\text{AsO}_4]_2 \cdot 8 \text{H}_2\text{O}$  and sample **3**, zeunerite,  $\text{Cu}[\text{UO}_2\text{AsO}_4]_2 \cdot 12 \text{H}_2\text{O}$ , at 15 K.

Edge, $\beta$	Shell	$R_{\text{EXAFS}}$ [ $\text{\AA}$ ] <sup>a</sup>	$N^b$	$\sigma^2$ [ $\text{\AA}^2$ ]	$\Delta E_0$ [eV]
Cu K, 45° sample <b>1</b>	Cu–OW <sub>CuI</sub>	1.94	2.4(1)	0.0018	–13.9
	Cu–O <sub>ax</sub>	2.46	1.2(1) <sup>d</sup>	0.0018 <sup>d</sup>	
	Cu–U'	4.04	0.8(1)	0.002 <sup>c</sup>	
	Cu–U''	4.52	0.7(1) <sup>c</sup>	0.002 <sup>c</sup>	
	Cu–As	4.84	1.6(2)	0.002 <sup>c</sup>	
Cu K, 45° sample <b>3</b>	Cu–OW <sub>CuI</sub>	1.94	3.1(2)	0.0016	–4.4
	Cu–O <sub>ax</sub>	2.46	1.1(2)	0.0016 <sup>d</sup>	
	Cu–U	4.22	1.3(5)	0.0013	
	Cu–U <sub>MS</sub>	4.22 <sup>d</sup>	2.7 <sup>d</sup>	0.0026 <sup>d</sup>	

a: Errors in distances  $R$  are  $\pm 0.02 \text{\AA}$

b: Errors in coordination numbers  $N$  are  $\pm 25\%$  with standard deviations in parentheses,  $\sigma^2$  – Debye-Waller factor,  $\beta$  – angle between polarization vector  $\varepsilon$  and sample surface (see Fig. 1).

c: Value fixed during the fit.

d: Linked during the least-square refinement to the previous variable.

to a highly symmetric arrangement of the  $[\text{UO}_2\text{AsO}_4]_\infty$  layers relative to Cu. In contrast, the spectrum of sample 1 shows two FT peaks in that region. The first peak originates from one uranium atom at a distance of 4.04 Å. The second peak is caused by arsenic atoms at a distance of 4.84 Å and one uranium atom at a distance of 4.52 Å. These observations indicate that the arrangement of the  $[\text{UO}_2\text{AsO}_4]_\infty$  layers is less symmetrical with regard to the copper atom in meta-zeunerite.

### 3.1.4. EXAFS data in comparison to X-ray diffraction literature data

A comparison of the EXAFS bond distances of sample 1 with the corresponding values from crystal structure data of Hanic [1] given in Table 2 shows that the atomic distances between heavy atoms and neighboring oxygen atoms differ by about 0.1 Å. These differences exceed the error of the EXAFS measurements. In contrast, the atomic distances between heavy scatterers (U–U and U–As) determined by EXAFS agree well with the XRD data given in the literature. As it is sometimes observed in heavy-atom structures, the position of the heavy scatterers are correctly determined by XRD whereas the positions of the light atoms are incorrect.

## 3.2. X-ray diffraction investigations

### 3.2.1. X-ray Weissenberg photographs

As mentioned above sample 1 is an intergrown zeunerite/meta-zeunerite mineral. X-ray Weissenberg photographs of this sample that were obtained from the  $(h0l)$  and  $(h1l)$  zones show two X-ray reflection types. One reflection type consists of very sharp dots whereas the reflections of the second type are strongly broadened. The sharp reflections belong to zeunerite. The broad reflections originate from meta-zeunerite. Both groups of reflections are in distinct symmetry relations. The  $hk0$  reflections are completely overlapped and some  $hkl$  reflections are only partly overlapped because of the similarity of their a lattice constants. The intergrowth relationship of both structures can be described with the relation  $\langle 001 \rangle$  zeunerite  $\parallel$   $\langle 001 \rangle$  meta-zeunerite and  $\langle 100 \rangle$  zeunerite  $\parallel$   $\langle 100 \rangle$  meta-zeunerite. The sharpness of the zeunerite reflections and the broad meta-zeunerite reflections shows that zeunerite is formed initially and meta-zeunerite domains grow as a secondary dehydration product according to defined intergrowth relationships to zeunerite. The observed reflection broadening in meta-zeunerite is a result of structural disorder originating from the

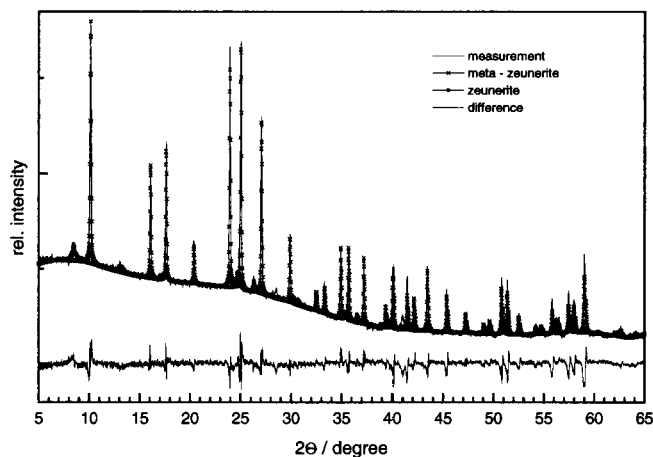


Fig. 5. X-ray powder diffraction pattern ( $\text{CuK}\alpha$  radiation) of copper uranyl arsenate sample 1.

phase transition from zeunerite to meta-zeunerite. This transition starts at the rim of the crystal. It seems that this phase transition is more developed for small crystals than for larger crystals.

### 3.2.2. X-ray powder diffraction measurements

The main part of the observed and calculated X-ray powder diffraction pattern of sample 1 is depicted in Fig. 5. This pattern shows the appearance of zeunerite and meta-zeunerite as in the Weissenberg photographs. Table 4 gives fit parameters and calculated lattice constants. The lattice constants of meta-zeunerite given in the literature are  $a = 7.13$  Å and  $c = 8.83$  Å [6] or  $a = 7.10$  Å and  $c = 17.42$  Å [7]. The powder pattern show very weak  $hkl$  reflections with the condition  $l = 2n + 1$  which corresponds to the large  $c$  lattice constant. But these weak reflections are not observed for all investigated single crystals (see below). The lattice constants of zeunerite agree with the values  $a = 7.18$  Å and  $c = 20.79$  Å given in the literature [7]. Because of uncertainties using the broad reflection profiles in the single-crystal measurements, the lattice constants are taken from the powder diffraction data. A quantitative phase analysis concerning the zeunerite/meta-zeunerite relation was performed using the atom coordinates of a single-crystal structure analysis as described below. Due to their layer structures, zeunerite and meta-zeunerite show the preferred orientation  $[001]$ . The analysis indicates that the powdered small crystal from sample 1 consists to 88.1% of meta-zeunerite and to 11.9% of zeunerite (Table 4), respectively.

Parameters	$\text{Cu}[\text{UO}_2\text{AsO}_4]_2 \cdot 12 \text{H}_2\text{O}$	$\text{Cu}[\text{UO}_2\text{AsO}_4]_2 \cdot 8 \text{H}_2\text{O}$
Lattice constants a, b	7.1751 Å	7.1065 Å
c	20.8728 Å	8.7095 Å
Profile function	PseudoVoigt 1	PseudoVoigt 1
$n_a$	0.77	0.494
Scaling factor	0.227	1.68
Mass fraction	11.9	88.1
Preferred orientation vector $H_p$	[001]	[001]
Orientation parameter $G$	1.240	1.101

Table 4. Quantitative phase analysis of sample 1 using the program PowderCell [14].

**Table 5.** Atomic coordinates and equivalent isotropic displacement parameters for zeunerite,  $\text{Cu}[\text{UO}_2\text{AsO}_4]_2 \cdot 12 \text{H}_2\text{O}$ , with  $a = 7.1751 \text{ \AA}$ ,  $c = 20.8728 \text{ \AA}$  and  $I4/mmm$ .  $U_{\text{eq}}$  is defined as one third of the trace of the orthogonalized  $U_{ij}$  tensor.

Atom	Site	Occupation	$x$	$y$	$z$	$U_{\text{eq}}$
U	4e	1.0	0	0	0.2948(1)	0.013(1)
As	4d	1.0	0	$-\frac{1}{2}$	$\frac{1}{4}$	0.017(1)
Cu1	2b	0.85	0	0	$\frac{1}{2}$	0.015(1)
Cu2	4e	0.075	0	0	0.1210(13)	0.015(1)
O1 <sub>ax</sub>	4e	1.0	0	0	0.3825(6)	0.029(3)
O2 <sub>ax</sub>	84e	1.0	0	0	0.2099(6)	0.026(3)
O <sub>eq</sub>	32o	0.5	0.0407(13)	0.3185(13)	0.2983(3)	0.025(3)
OW <sub>Cu1</sub>	16l	0.5	-0.0160(5)	-0.2691(16)	$\frac{1}{2}$	0.035(3)
OW <sub>Cu2</sub>	32o	0.5	0.2354(14)	-0.4163(13)	0.5868(6)	0.032(2)

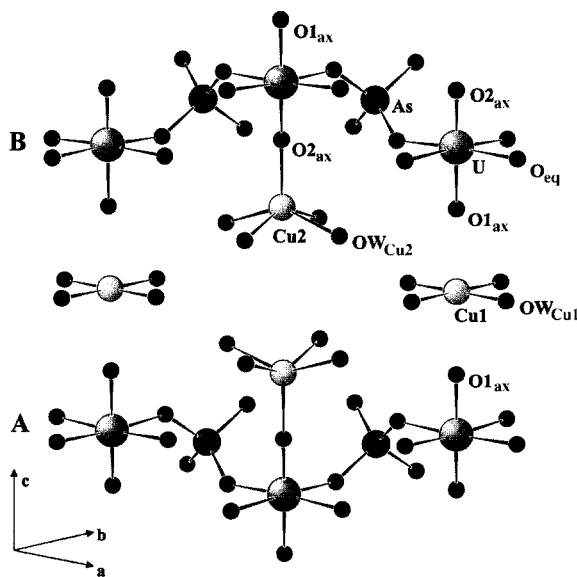


**Fig. 6.** A segment of the zeunerite structure.

### 3.2.3. Single-crystal diffraction

#### a. Zeunerite

The atomic coordinates and equivalent isotropic displacement parameters of zeunerite,  $\text{Cu}[\text{UO}_2\text{AsO}_4]_2 \cdot 12 \text{H}_2\text{O}$ , are given in Table 5. Bond lengths and angles are given in Table 8. A simplified picture of the zeunerite crystal structure is shown in Fig. 6. The symmetry of the reflection intensity distribution is  $I4/mmm$ . But this may be caused

alone by the heavy atoms and the axially positioned oxygen atoms. If the structure refinement is performed in the space group  $I4/m$ , an ordered structure picture appears. In order to achieve a convenient convergence, it is necessary to treat the crystal as a twin with the matrix (010 100 001) and volume fractions of nearly 50%. But the equatorial oxygen atoms show a tendency to split at the time in two positions. This indicates the existence of a higher symmetry. An analysis of zeunerite in the space group  $I4/mmm$  leads to a structure picture with a disorder of layer packages. The atom parameters resulting from both refinements are almost equal. The calculation in the space group  $I4/mmm$  gives  $R1(\text{on } F) = 0.037$  whereas a refinement in the space group  $I4/m$  gives a resulting  $R1(\text{on } F) = 0.051$ . Due to the better  $R$  value, the structure of zeunerite is presented in the space group  $I4/mmm$ .

In the structure of zeunerite, the  $[\text{UO}_2\text{XO}_4]_{\infty}$  sheets follow each other in an ABAB sequence (Fig. 6). Thus, two different interlayer cavity types exist in the structure. The copper atoms are found in two different positions with individual occupation factors. Copper atom Cu1 is surrounded by four water molecules in a square planar arrangement and has an occupation factor of 0.85. The second copper atom, Cu2, is also surrounded by four water molecules. But Cu2 is shifted out of its common plane and forms a square pyramidal configuration with the oxygen atoms. This position has only an occupation factor of 0.075. Uranium is located at a special position on the fourfold rotation axis. Due to the chosen space group  $I4/mmm$ , the mirrors virtualise double oxygen posi-

**Table 6.** Atomic coordinates and equivalent isotropic displacement parameters for meta-zeunerite (ordered),  $\text{Cu}[\text{UO}_2\text{AsO}_4]_2 \cdot 8 \text{H}_2\text{O}$ , with  $a = 7.1065 \text{ \AA}$ ,  $c = 17.4195 \text{ \AA}$  and  $P4/nmc$ .  $U_{\text{eq}}$  is defined as one third of the trace of the orthogonalized  $U_{ij}$  tensor.

Atom	Site	Occupation	$x$	$y$	$z$	$U_{\text{eq}}$
U	4c	1.0	$\frac{1}{4}$	$\frac{1}{4}$	0.4448(1)	0.015(1)
As	4b	1.0	$-\frac{1}{4}$	$\frac{1}{4}$	$\frac{1}{2}$	0.017(1)
Cu1	4c	0.5	$\frac{1}{4}$	$\frac{1}{4}$	0.6892(5)	0.021(2)
O1 <sub>ax</sub>	4c	1.0	$\frac{1}{4}$	$\frac{1}{4}$	0.5473(11)	0.017(4)
O2 <sub>ax</sub>	4c	1.0	$\frac{1}{4}$	$\frac{1}{4}$	0.3429(12)	0.018(4)
O <sub>eq</sub>	16g	1.0	0.1987(14)	-0.4330(16)	0.4410(5)	0.008(2)
OW <sub>Cu1</sub>	16g	1.0	0.1890(20)	-0.0180(20)	0.6913(7)	0.028(3)

**Table 7.** Atomic coordinates and equivalent isotropic displacement parameters for meta-zeunerite (disordered),  $\text{Cu}[\text{UO}_2\text{AsO}_4]_2 \cdot 8 \text{H}_2\text{O}$ , with  $a = 7.1065 \text{ \AA}$ ,  $c = 8.7095 \text{ \AA}$  in  $P4/nmm$ .  $U_{\text{eq}}$  is defined as one third of the trace of the orthogonalized  $U_{ij}$  tensor.

Atom	Site	Occupation	$x$	$y$	$z$	$U_{\text{eq}}$
U	2c	1.0	$\frac{1}{4}$	$\frac{1}{4}$	0.8896(1)	0.014(1)
As	2a	1.0	$-\frac{1}{4}$	$\frac{1}{4}$	1	0.016(1)
Cu1	2c	0.5	$\frac{1}{4}$	$\frac{1}{4}$	1.3783(4)	0.021(1)
O1 <sub>ax</sub>	2c	1.0	$\frac{1}{4}$	$\frac{1}{4}$	1.0944(11)	0.017(2)
O2 <sub>ax</sub>	2c	1.0	$\frac{1}{4}$	$\frac{1}{4}$	0.6859(12)	0.017(2)
O <sub>eq</sub>	16k	0.5	-0.1995(11)	0.4330(12)	1.1157(7)	0.019(2)
OW <sub>Cu1</sub>	16k	0.5	0.1870(20)	0.5169(15)	1.3836(8)	0.056(6)

**Table 8.** Selected atomic distances [Å] and angles [°] for zeunerite,  $\text{Cu}[\text{UO}_2\text{AsO}_4]_2 \cdot 12 \text{H}_2\text{O}$ , ordered and disordered meta-zeunerite,  $\text{Cu}[\text{UO}_2\text{AsO}_4]_2 \cdot 8 \text{H}_2\text{O}$ . For the sake of simplicity symmetry codes are left out.

	Zeunerite	Meta-zeunerite (ordered)	Meta-zeunerite (disordered)
U–O <sub>1ax</sub>	1.830(13)	1.786(19)	1.784(9)
U–O <sub>2ax</sub>	1.772(12)	1.774(21)	1.774(10)
U–O <sub>eq</sub>	2.305(9)	2.283(11)	2.282(8)
U–As	3.707(2)	3.681(1)	3.681(1)
U–U	5.407(1)	5.380(1)	5.380(1)
As–O <sub>eq</sub>	1.673(9)	1.697(11)	1.684(2)
Cu1–OW <sub>Cu1</sub>	1.934(12)	1.954(14)	1.949(3)
Cu1–O <sub>1ax</sub>	2.453(13)	2.472(21)	2.473(10)
Cu1–O <sub>2ax</sub>	–	2.677(23)	2.679(11)
Cu2–OW <sub>Cu2</sub>	2.12(13)	–	–
Cu2–O <sub>2ax</sub>	1.866(31)	–	–
O <sub>1ax</sub> –U–O <sub>2ax</sub>	180	180	180
O <sub>1ax</sub> –U–O <sub>eq</sub>	88.17(15)	91.65(24)	91.15(15)
O <sub>2ax</sub> –U–O <sub>eq</sub>	91.83(15)	88.35(24)	88.85(15)
O <sub>eq</sub> –As–O' <sub>eq</sub>	111.3(3)	111.5(3)	111.0(2)
O <sub>eq</sub> –As–O'' <sub>eq</sub>	105.8(5)	105.5(7)	106.1(5)

tions. Cu1 is located at the mirror plane *m*. (Wykoff position 4b). In accordance with this symmetry relation, the FT of the Cu K-edge EXAFS spectra from the sample **3** shows only one significant peak of the Cu–U scattering pair (Fig. 4). The deviation between the Cu–U distance determined by XRD (4.28 Å) and EXAFS (4.22 Å) may be caused by the temperature difference during the measurements.

### b. Meta-Zeunerite

For meta-zeunerite,  $\text{Cu}[\text{UO}_2\text{AsO}_4]_2 \cdot 8 \text{H}_2\text{O}$ , the atomic coordinates and equivalent isotropic displacement parameters are given in Table 6 and 7. Bond lengths and angles are given in Table 8. The main structure motif of meta-zeunerite is depicted in Fig. 7. The XRD measurement using sample **2** shows very weak *hkl* reflections with the condition  $l = 2n + 1$ . They are similar to those found in the X-ray powder diffraction data of sample **1**. These weak reflections are not observed in each analyzed sample piece. From these findings one can conclude that meta-zeunerite can crystallize with a different degree of disorder depend-

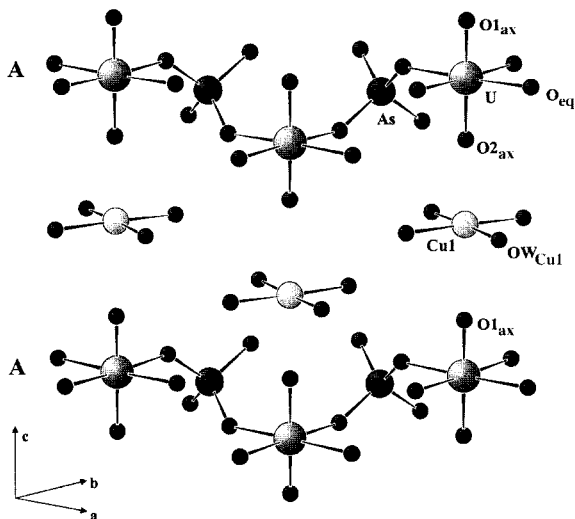


**Fig. 7.** A segment of the meta-zeunerite structure.

ing on the layer arrangement. Taking into account the observation that the degree of disorder varies within different crystal regions, the structure determination of meta-zeunerite in the ordered as well as in the disordered form is presented in this paper. Using a lattice constant of  $c = 8.7095 \text{ Å}$  and space group  $P4/nmm$ , the sequence of the possible layer arrangements is completely statistical. A fully ordered structure can be described by the space group  $P4/ncc$  and  $c = 17.4195 \text{ Å}$ . All systematically weak reflections are disregarded in the refinement of the disordered structure. The final  $R$ (on  $F$ ) value for this structure analysis is 0.029. A  $R$  value 0.058 is obtained when the refinement procedure is performed in the space group  $P4/ncc$  with doubled  $c$  constant. This higher  $R$  value might be anticipated for purely statistical reasons because of the use of systematically weak reflections. Nevertheless, the resulting bond lengths and angles of the superposition structure in the space group  $P4/nmm$  seem to be more precise because of their much lower estimated standard deviations. The broad reflections in meta-zeunerite appear to be related to stacking faults in the [001] direction, giving ordered and disordered structure domains.

In the meta-zeunerite structure, the  $[\text{UO}_2\text{AsO}_4]_\infty$  sheets follow each other in an AAA sequence (Fig. 7). The sheets are packed more closely together. This reduces the interlayer cavity volume which is related to a decrease in the water content from 12  $\text{H}_2\text{O}$  in zeunerite to 8  $\text{H}_2\text{O}$  in meta-zeunerite. Only one interlayer cavity type exists in the meta-zeunerite structure. The bond lengths and angles within the uranyl arsenate sheet are not influenced significantly by the phase transition from zeunerite to meta-zeunerite. In the meta-zeunerite structure, the interlayer space between the  $[\text{UO}_2\text{AsO}_4]_\infty$  sheets consists of a two-dimensional network of water molecules. Four water molecules are arranged in squares and centered by a  $\text{Cu}^{2+}$  cation. Statistically half of the equivalent positions are occupied. In meta-zeunerite only one symmetrically independent Cu position exists.  $\text{Cu}^{2+}$  is located at the Wykoff position 4c with a free  $z$  parameter. In the direction of the  $z$  axis, there are two symmetrically independent oxygen atoms, O<sub>1ax</sub>, at a distance of 2.47 Å and O<sub>2ax</sub> at 2.68 Å, respectively. There are two uranium atoms at distances of 4.25 Å and 4.45 Å and four arsenic atoms at a distance of 4.85 Å. This is in agreement with the FT of the Cu K-edge EXAFS spectrum of sample **1** (Fig. 4), which shows two significant peaks caused by two symmetrically inequivalent uranium positions and one closer located arsenic atom. There are noticeable differences between the atomic distances measured by EXAFS at low temperature and XRD measured at room temperature. These structural modifications may be caused by a shift of the Cu atom at low temperature in connection with a reduction of the space group symmetry comparable to the structural change of  $\text{D}[\text{UO}_2\text{AsO}_4] \cdot 4 \text{D}_2\text{O}$  from the space group  $P4/nnc$  at 305 K [16] to  $P\bar{1}$  at 4 K [21].

### Conclusions

Depending on a disorder effect, the XRD results gave two space group symmetries,  $P4/ncc$  for ordered and  $P4/nmm$

for disordered  $\text{Cu}[\text{UO}_2\text{AsO}_4]_2 \cdot 8 \text{H}_2\text{O}$ , respectively. For comparison, the literature reports space group  $P4_2/nmc$ . The bond distances obtained by EXAFS (Table 2) agree well with the distances calculated using the completely revised structure of  $\text{Cu}[\text{UO}_2\text{AsO}_4]_2 \cdot 8 \text{H}_2\text{O}$  (Table 8). These results demonstrate that EXAFS spectroscopy allows a precise analysis of local bond lengths in the environment of heavy atoms. Furthermore, since EXAFS is sensitive to the short-range order only, it is possible to study crystal material of poor quality or materials with disordering effects like meta-zeunerite. EXAFS measurements provide an independent criterion for the accuracy or inaccuracy of crystal structure parameters.

The atomic distances in the  $[\text{UO}_2\text{AsO}_4]_\infty$  layers are identical in zeunerite and meta-zeunerite within the experimental error limits. Low temperature EXAFS measurements point to a different symmetry in the sheet arrangement in zeunerite and meta-zeunerite. In zeunerite, the uranyl atoms are arranged with symmetric relation with regard to the Cu interlayer atom, whereas in meta-zeunerite this symmetry is lost. These results agree with the crystal structure given by XRD measurements. They showed that main structural differences between zeunerite and meta-zeunerite arise in the arrangement of the uranyl arsenate sheets. The intergrowth relationship between zeunerite and meta-zeunerite and the effect of reflex broadening during the phase transition indicate that meta-zeunerite grows in nature by to dehydration of zeunerite.

**Acknowledgments.** The copper uranyl arsenate sample **1** is stored at the Staatliches Museum für Mineralogie und Geologie, Dresden, collection number 21004Sy. The second crystal **2** used from the mine "Weißer Hirsch" at Schneeberg/Saxony in Germany originated from the Institut für Mineralogie, Kristallographie und Materialwissenschaft, Leipzig, with the collection number 10525. We thank M. Acker for the synthesis of sample **3**, H. Funke and U. Strauch for technical support. We acknowledge the European Synchrotron Radiation Facility for provision of synchrotron radiation.

## References

- [1] Hanic, F.: The crystal structure of meta-zeunerite  $\text{Cu}(\text{UO}_2)_2(\text{AsO}_4)_2 \cdot 8 \text{H}_2\text{O}$ . Czech. J. Phys. **B10** (1960) 169–181.
- [2] Thompson, H. A.; Brown, G. E.; Parks, G. A.: XAFS spectroscopic study of uranyl coordination in solids and aqueous solution. Am. Mineral. **82** (1997) 483–496.
- [3] Bruns, P. C.; Miller, M. L.; Ewing, R. C.:  $\text{U}^{6+}$  minerals and inorganic phases: a comparison and hierarchy of crystal structures. Canadian Min. **34** (1996) 845–880.
- [4] Weigel, F.: The carbonates, phosphates and arsenates of the hexavalent and pentavalent actinides. In: *Handbook on the Physics and Chemistry of the Actinides* (Eds. A. J. Freeman, C. Keller), p. 243–288. Elsevier Science Publishers, Amsterdam 1985.
- [5] Gaines, R. V.; Skinner, H. C. W.; Foord, E. E., Rosenzweig, A.: Dana's new mineralogy. John Wiley & Sons Inc., New York 1997.
- [6] Frondel, C.: Systematic mineralogy of uranium and thorium. Geol. Survey Bull. **1064** 1958.
- [7] Walenta, K.: Beiträge zur Kenntnis seltener Arsenatminerale unter besonderer Berücksichtigung von Vorkommen des Schwarzwaldes, 1. Folge. Tschermarks miner. petrogr. Mitt. **9** (1962) 111–174.
- [8] Vochten, R.; Goeminne, A.: Synthesis, crystallographic data, solubility and electrokinetic properties of meta-zeunerite, meta-kirchheimerite and nickel-uranylarsenate. Phys. Chem. Minerals **11** (1984) 95–100.
- [9] Matz, W.; Schell, N.; Bernhard, G.; Prokert, F.; Reich, T.; Claußner, J.; Oehme, W.; Schlenk, R.; Diemel, S.; Funke, H.; Eichhorn, F.; Betzl, M.; Pröhl, D.; Strauch, U.; Hüttig, G.; Krug, H.; Neumann, W.; Brendler, V.; Reichel, P.; Denecke, M. A.; Nitsche, H.: ROBL – a CRG beamline for radiochemistry and materials research at the ESRF. J. Synchrotron Rad. **6** (1999) 1076–1085.
- [10] Krolzig, A.; Materlik, G.; Swars, M.; Zegenhagen, J.: A feedback control system for synchrotron radiation double crystal instruments. Nucl. Instr. and Meth. **219** (1984) 430–434.
- [11] Bucher, J. J.; Allen, P. G.; Edelstein, N. M.; Shuh, D. K.; Madden, N. W.; Cork, C.; Luke, P.; Pehl, D.; Malone, D.: A multi-channel monolithic Ge detector system for fluorescence X-ray absorption spectroscopy. Rev. Sci. Instr. **67** (1996) 1–4.
- [12] Kraft, S.; Stümpel, J.; Becker, P.; Kuetgens, U.: High resolution X-ray absorption spectroscopy with absolute energy calibration for the determination of absorption edge energies. Rev. Sci. Instrum. **67** (1996) 681–687.
- [13] George, G. N.; Pickering, I. J.: EXAFSPAK, a suite of computer programs for analysis of X-ray absorption spectra. Stanford Synchrotron Radiation Laboratory, Stanford 1995.
- [14] Kraus, W.; Nolze, G.: PowderCell as a teaching tool, CPD Newsletter **20** (1998) 274.
- [15] Ankudinov, A. L.; Ravel, B.; Rehr, J. J.; Conradson, S. D.: Real-space multiple-scattering calculation and interpretation of X-ray-absorption near-edge structure. Phys. Rev. **B58** (1998) 7565–7576.
- [16] Fitch, A. N.; Bernard, L.; Howe, A. T.; Wright, A. F.; Fender, B. E. F.: The room-temperature structure of  $\text{DUO}_2\text{AsO}_4 \cdot 4 \text{D}_2\text{O}$  by powder neutron diffraction. Acta Cryst. **C39** (1983) 159–162.
- [17] Hennig, C.; Nolze, G.: Characterization of the preferred orientation in EXAFS-samples using Bragg-Brentano X-ray diffraction. In: *Speciation, techniques and facilities for radioactive materials at synchrotron light sources*, p. 235–243. Workshop Proceedings, Grenoble 1998, Publisher: NEA/OECD Paris 1999.
- [18] Stöhr, J.; Jaeger, R.: Polarization-dependent phase and amplitude interference effects in the  $L_{2,3}$  surface extended X-ray absorption fine structure. Phys. Rev. **B27** (1983) 5146–5149.
- [19] Hennig, C.; Reich, T.; Funke, H.; Rossberg, A.; Rutsch, M.; Bernhard, G.: EXAFS as a tool for bond-length determination in the environment of heavy atoms. J. Synchr. Rad. **8** (2001) 695–697.
- [20] Calos, N. J.; Kennard, C. H. L.: Crystal structure of copper bis(uranyl phosphate) octahydrate (metatorbernite),  $\text{Cu}(\text{UO}_2\text{PO}_4)_2 \cdot 8 \text{H}_2\text{O}$ . Z. Krist. **211** (1996) 701–702.
- [21] Fitch, A. N.; Bernard, L.; Howe, A. T.; Wright, A. F.; Fender, B. E. F.: The structure of  $\text{UO}_2\text{DAsO}_4 \cdot 4 \text{D}_2\text{O}$  at 4 K by powder neutron diffraction. Acta Cryst. **B39** (1982) 2546–2554.